Mapping of Soil Moisture Variability, Using the Sentinel-2 Data Optical-Trapezoid Approach

Malgorzata Verőné Wojtaszek[1] and László Vass[2]

[1]Alba Regia Technical Faculty, Obuda University, Pirosalma u. 1-3, 8000 Székesfehérvár, Hungary, wojtaszek.malgorzata@amk.uni-obuda.hu

[2]Deputy head of the Hydrographic Department, Lower Danube Valley Water Management Directorate, Széchenyi István út 2/c, 6500 Baja, Hungary, vas.laszlo@aduvizig.hu

Abstract: Understanding soil moisture is crucial in various aspects of daily life and scientific pursuits. Among these, knowledge about water stress conditions holds particular significance for both agriculture and soil conservation. The objective of this research is to explore the application of satellite imagery in the cartography and surveillance of moisture levels within an agricultural region. Soil moisture content was assessed using the optical trapezoid model (OPTRAM). Developed by Sadeghi et al. (2015), the OPtical TRApezoidal model (OPTRAM) was designed to gauge soil water content (SWC) by assuming a linear correlation between soil moisture content and shortwave transformed reflectance (STR). The parameters essential for calculating moisture content were identified by scrutinizing pixel distribution in the STR-NDVI (Normalized Difference Vegetation Index) space. The examination period spanned from April to October 2021. The models were employed to compute the spatial fluctuation of soil moisture and its deviation for three satellite images during the summer of 2021.

The study site was located in Hungary's Bács-Kiskun county, encompassing agricultural fields with a total expanse of 5500 km2. The study region exhibited variability in terms of soil composition and topography. Meteorological parameters recorded at 19 stations within a drought monitoring network, along with soil moisture measurements at different depths, were also taken into account. To validate the data obtained from the soil moisture sensor and model, soil samples were collected at a depth of 10 cm for laboratory moisture assessments. The present condition can be depicted through the analysis of a spatial image, while time series analyses enable continuous monitoring of soil moisture. The eCognition software environment, employing the object-based (OBIA) approach, was used to process satellite data. Statistical methods were utilized to establish correlations between the datasets measured at the site and estimated from satellite images.

Keywords: satellite images; Sentinel2; image processing; soil moisture; OPTRAM model; eCognition

1 Introduction

Up-to-date data of soil moisture are crucial in various aspects of daily life and scientific endeavors. Notably, information about water stress conditions holds particular significance for agriculture and soil conservation. Water stands as a pivotal factor in agriculture, playing an essential role throughout the entire crop growth cycle. It is indispensable for seed germination, acts as a carrier for the distribution of mineral nutrients, and is closely linked to biomass production [1]. Extreme weather events can pose challenges, even leading to the complete destruction of plants. Excessively high soil moisture hinders access to agricultural areas and poses harm to crops, while insufficient soil moisture also damages crops, necessitating irrigation.

Weather factors, especially precipitation and air temperature, significantly influence agricultural outcomes. Crops are susceptible to the detrimental impacts of drought, particularly during periods of exceptionally low precipitation or extremely high temperatures. Monitoring soil moisture becomes instrumental in tracking drought conditions. Conventional approaches, dependent on data gathered from handheld or field sensors, as well as soil sampling and laboratory analysis, offer point-specific information, struggling to effectively capture the temporal and spatial fluctuations in soil moisture within agricultural fields. These methods are characterized by being time-consuming, labor-intensive, and challenging to automate due to the heterogeneous nature of soil and crop cover. Providing point-specific information, these approaches offer limited insights into the field status and prove challenging to scale up to plant, field, or regional levels [2] [3], making them unsuitable for effective monitoring.

Due to increasingly better spatial, spectral, and temporal resolution of satellite systems, continuous monitoring of Earth becomes achievable. Currently available remote sensing technologies can be applied to map the water balance of plants. A typical example of this is measuring the surface temperature in the thermal infrared spectrum or using microwave radiation to assess soil moisture. Furthermore, the use of spectral vegetation indices allows the study of how the canopy reflects environmental changes. Based on previous studies, it can be stated that soil reflectance in the optical range [4] [5], thermal radiation [6] [7], and microwave backscatter [8] [9] show a high correlation with soil moisture content. Surveying methods based on optical, thermal, and microwave remote sensing of soil moisture are available in the literature. Numerous studies rely on the calculation and analysis of spectral indices, revealing a clear connection between reflectance values and canopy changes induced by water stress.

The objective of this research was to explore the application of remote sensing data for mapping soil moisture variability within an agricultural region. The Optical Trapezoid Model (OPTRAM) was used to calculate the spatial fluctuations in soil moisture and its variation across three satellite images from the summer of 2021. The study period spanned from April to October 2021. Meteorological data from 19 stations within a drought monitoring network, along with soil moisture measurements at various depths, were also analyzed. To validate the sensor- and model-based soil moisture data, soil samples were collected at a depth of 10 cm for laboratory moisture assessment.

2 Study Area

Moisture retrievals for the study site were derived from a location situated in the southern region of Hungary (Figure 1), specifically within Bács-Kiskun county on the Great Hungarian Plain. According to the topographic map, the highest point in the area is at an altitude of 174 meters above sea level (m.a.s.l.), while the lowest point is at 84 m.a.s.l [10]. From a topographical perspective, the study area can be classified into two parts. The region between the Main Canal of the Danube Valley and the Danube itself constitutes a floodplain, while the eastern part is a lowland plain. The study area exhibits a variety of soil types, with more than 10 types identified. Predominantly, different chernozemic soil types (HSCS: Hungarian Soil Classification System) characterize the largest areas, featuring an organic carbon content ranging from 1.00% to 2.99% [11]. Meadow soils and saline soils are common in the valleys, primarily utilized as arable land due to their favorable agricultural characteristics.

The soil moisture in the floodplain section of the study area is influenced by both subsurface water and precipitation. In contrast, on the lowland plain section, it is solely dependent on precipitation.

The land cover is dominated by agricultural lands, its share is 51%. The second largest land cover category is forest, while the third category is pasture. Forests and pastures can be found primarily on the lowland plain.

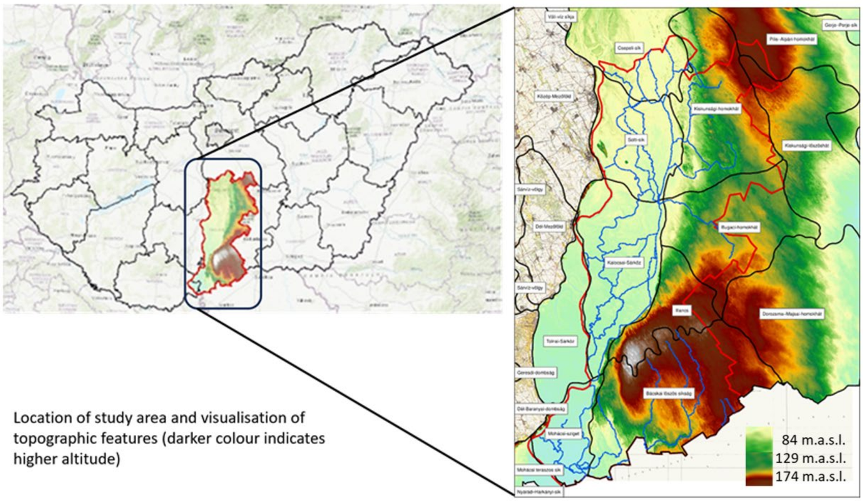

Figure 1
Location of the area under study in Hungary, visualization of topographic features (outlined with red line, topography inside)

3 Method

The prevailing methodology for Remote Sensing (RS) of soil moisture often employs widely used models like the "trapezoid" or "triangle," which integrate both optical and thermal data. One such model, known as the Thermal-Optical Trapezoid Model (TOTRAM), utilizes the pixel distribution within the feature space created by land surface temperature values (thermal band) and vegetation index values (VIS, IR bands) [12] [13]. TOTRAM has demonstrated efficacy in estimating surface soil moisture, and various modified versions have adapted to advancements in optical sensor technologies. With the progression of optical sensors in the spectrum range, models now integrate additional and superior data. Optical remotes sensing based data, including indices derived from the Red-Near-infrared (R-NIR) triangular space, such as the Perpendicular Drought Index (PDI) [14], Distance Drought Index (DDI) [15], and the Triangle Soil Moisture Index, have become prominent. In such studies, the short-wave infrared (SWIR) range is gaining prominence, as evidenced by the development of indices parameterized by the SWIR (instead of thermal) and near-infrared (NIR) trapezoidal space. Examples include the Shortwave Perpendicular Drought Index (SPDI) [16] and the Modified Shortwave Infrared Perpendicular Drought Index (MSPDI) [17].

As a result of the research by Sadeghi et al. [18], a new model, the Optical Trapezoidal Model (OPTRAM), has been introduced. This model is based on the correlation between soil moisture and shortwave infrared (SWIR) transformed reflectance, with the authors assuming a linear relationship between the two variables. The theoretical foundation and application of OPTRAM, using Sentinel-2 and Landsat OLI satellite imagery, were presented in 2017. Since then, the method has been applied in various research projects [19] [20].

In contrast to the traditional trapezoid model, TOTRAM, which relies on pixel distribution within the feature space of surface temperature and vegetation index (LST-VI) and assumes an inverse linear relationship between surface soil moisture and LST (Figure 2), the Optical Trapezoid Model (OPTRAM) was specifically developed for Soil Water Content (SWC) estimation using optical satellite data. OPTRAM is based on the linear physical relationship between soil moisture and Shortwave Infrared Transformed Reflectance (STR) [18].

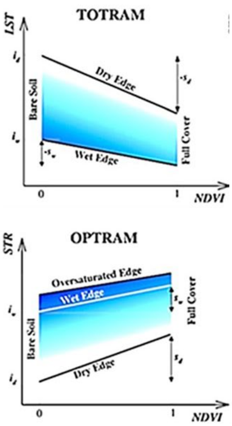

$STR_d = i_d + s_d NDVI$

$STR_w = i_w + s_w NDVI$

where STR_d and STR_w are the STR at θ_d and θ_w

θ_d: local minimum dry soil moisture content

θ_w: local maximum wet soil moisture content

$$W = \frac{i_d + s_d NDVI - STR}{i_d - i_w + (s_{d-s_w})NDVI}$$

where i_d, s_d, and i_w, s_w are dry and wet edges parameters.

Figure 2

Illustrating the theoretical background of the Thermal-Optical Trapezoid Model (TOTRAM) and the Optical Trapezoid Model (OPTRAM) [16]

OPTRAM necessitates parameterization at a specific location, determined by the pixel distribution within the STR-NDVI space (Figure 2). In this context, R refers to reflectance, STR refers to Shortwave Infrared Transformed Reflectance and is defined as follows:

$$STR = \frac{(1 - R_{SWIR})^2}{(2 * R_{SWIR})} \tag{1}$$

The parameters used in the calculation can be derived for a particular location by extracting information from the dry and wet edges of the optical trapezoid illustrated in Figure 2.

During the research and OPTRAM model run, the equation coefficients (Figure 2) were derived from the pixel distribution within the STR-NDVI space. The model was then executed individually for each available image, and an integrated trapezoid was defined to encompass the pixel distribution of all selected images. This integrated trapezoid was used to assess the overall parameterization. During the work dry (i_d and s_d) and wet (i_w and s_w) edges were determined by visual inspection of the STR-NDVI spaces so that the trapezoids surrounded the majority of the pixels. From i_d and s_d (dry edge parameters) and i_w and s_w (wet edge parameters), the normalized moisture content (W) was estimated for each pixel based on the equations summarized in the figure above (Figure 2).

4 Data Acquisition and Analysis

4.1 Field Data Acquisition

In this study, meteorological and soil moisture data were obtained from weather stations, supplemented by soil samples collected for laboratory analysis. The study area comprises 19 stations, with two in operation since 2018, sixteen since 2019, and one since 2021. These stations are strategically located within 2.5x2.5 m fenced areas on cultivated land, predominantly ploughland, occasionally extending to meadows or pastures. Within each fenced area, a central column supports various instruments, including the weighting rain gauge (OTT Pluvio 2), soil moisture sensors (Figure 3), temperature sensors (Decagon 5 TM), a solar panel, a buffer accumulator, and a combined air temperature and humidity sensor (ADCON TR1). The weather stations primarily measure temperature, humidity, wind speed and direction, rainfall, and air pressure, totaling nine parameters. Data are collected hourly and transmitted to the data acquisition server every 3-6 hours. Soil moisture and soil temperature are measured at depths of 10 cm, 20 cm, 30 cm, 45 cm, 60 cm and 75 cm.

The soil sensors are highly sensitive electromagnetic induction measurement devices that gauge near-surface electromagnetic conductivity. The 5TM determines volumetric water content (VWC) by assessing the dielectric constant of the soil using capacitance/frequency domain technology. The sensor emits a 70 MHz oscillating wave to the sensor prongs, which charges based on the dielectric of the material. The stored charge is proportional to soil dielectric and soil volumetric water content (VWC). The 5TM microprocessor measures the charge and outputs a value of dielectric permittivity from the sensor. Soil moisture data from a network of drought monitoring stations in the study area was used for parameterization.

Figure 3
Example of the installed soil sensors

To validate the data obtained from the soil moisture sensor, soil samples were collected at a depth of 10 cm and subsequently processed in the laboratory. The relationship between the results obtained was investigated through correlation and regression analysis, revealing a correlation coefficient (R^2) of 0.85 between the sensor readings and the measured soil moisture values (Figure 4, Table 1).

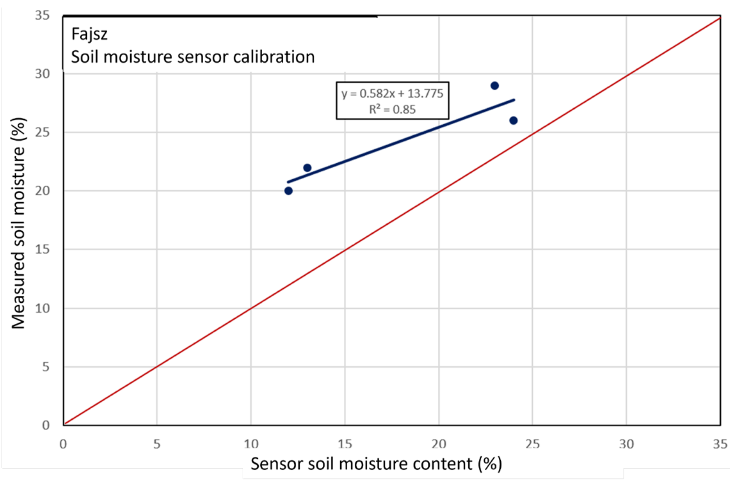

Figure 4
Soil moisture sensor calibration

Table 1
Soil moisture calibration coefficients

Station	Slope (m)	Axis cross-section (t)
Ósükösd	1.33	1.10
Fajsz	0.58	13.78
Kalocsa	1.58	-11.00
Homokmégy	1.28	-3.00

4.2 Satellite Images and Precipitation Data

In this study, we utilized multispectral imagery obtained from the European Space Agency's Sentinel-2 satellite, acquired through the ESA Sentinel Scientific Data Hub. The Sentinel-2 satellite offers high spatial resolution ranging from 10 to 60 meters, encompassing 13 spectral bands that span the visible (VIS), near-infrared (NIR), and shortwave infrared (SWIR) electromagnetic frequency domains. With a temporal resolution of approximately 5 days, the satellite observations were collected during the period between April and October 2021. To ensure data quality, only cloud-free images were considered initially. Subsequently, following a preliminary interpretation, three images were selected for further processing. The selection process took into account meteorological factors, specifically the amount and intensity of precipitation, as additional criteria for refining the dataset.

The study area and the periods of investigation were selected based on the spatial and temporal distribution of precipitation. In 2021, the lowest precipitation (413 mm) occurred in Fajsz; consequently, the focal area for the analyses encompassed Fajsz and the surrounding drought monitoring stations (Ósükösd: 424 mm, Kalocsa: 472 mm, Sandy Mountain: 488 mm). The study area is delineated by a red rectangle in Figure 5.

Analyses were conducted for two distinct periods, as highlighted in green in Figure 6. The OPTRAM model was employed to assess water conditions in the designated area during two contrasting weather phases: the aftermath of heavy rainfall in April 2021 and the dry spell in August 2021. The April period exhibits a notable peak in soil moisture levels, while the August period is characterized by relative aridity. Referencing Figure 6, the graph illustrates precipitation and soil moisture dynamics in the study region throughout the entire year of 2021, spanning from January to December. Notably, a significant rainfall event occurred in late May, leading to heightened soil water saturation. Despite minor precipitation occurrences between May and August, they had minimal impact on soil moisture content, resulting in its sustained low levels for approximately two months.

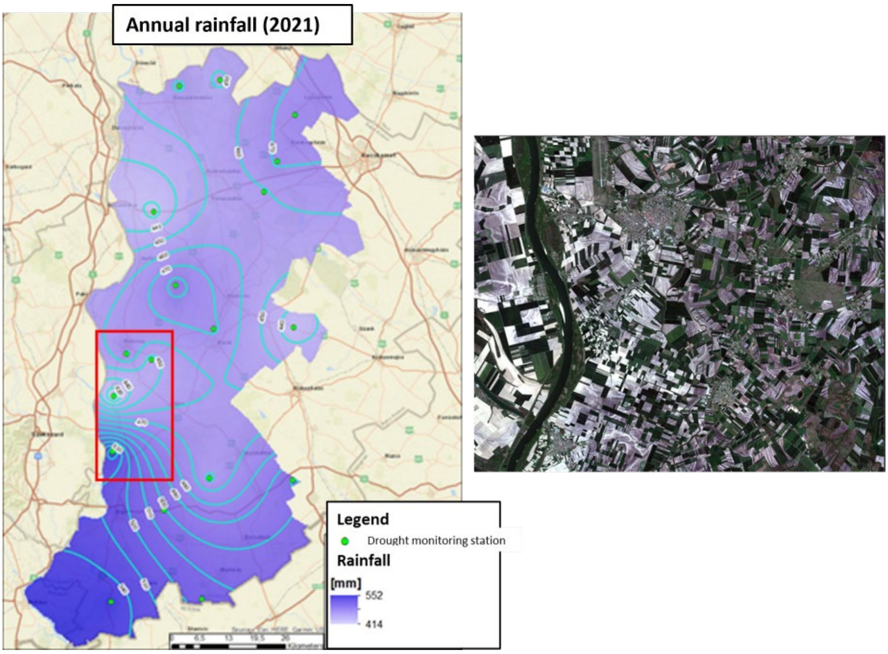

Figure 5

Spatial distribution of changes in annual rainfall (2021) and Sentinel2 (RGB) image for study area

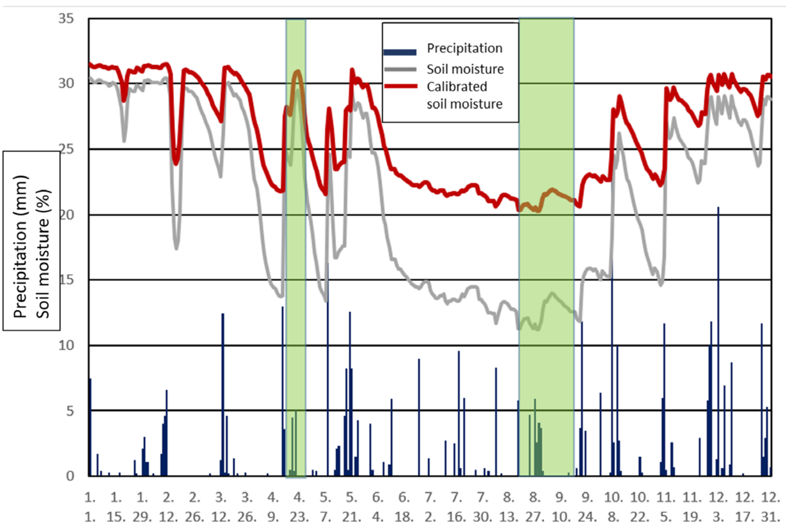

Figure 6

Time series (precipitation, soil moisture and calibrated soil moisture) of Fajszi station (2021)

4.3 Data Analysis

We used geospatial (QGIS) and image processing software to store and manage data from different sources and in different formats. Raster data analysis was conducted using the eCognition Developer software, with image processing and model application performed through object-based image analysis (OBIA). Figure 7 illustrates the workflow detailing the key steps in data analysis for mapping surface soil moisture with OPTRAM. The data extraction process encompasses several stages, including data pre-processing, multi-level image segmentation, feature extraction, index delimitation, and the application of the optical trapezoid model.

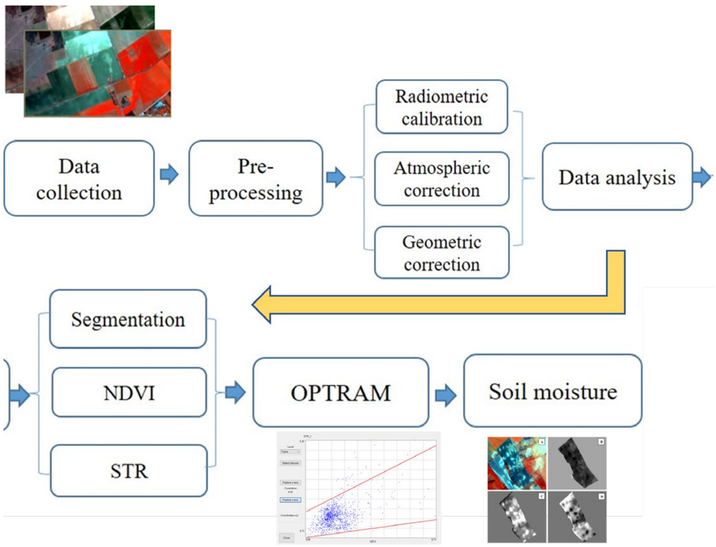

Figure 7
Diagram for satellite data analysis in soil moisture estimation by OPTRAM [1]

The Sentinel-2 images (Level-1C) downloaded from the Copernicus database come with radiometric and geometric corrections, including orthorectification. The Level-1C data represent surface reflectance measured at the top of the atmosphere (TOA). Data analysis was confined to the study area, employing a hierarchical framework to delineate the field of interest at the super-object level. The analysis was conducted at the sublevel, with the unit under consideration being 20 m, allowing for the determination of soil moisture values at 20 m intervals. After multi-level segmentation, we computed the requisite characteristics for each study unit to facilitate model execution, including vegetation indices such as the normalized differential vegetation index (NDVI) and short-wave infrared transformed reflectance (STR). In the context of water stress models, the NDVI serves as a widely utilized measure. NDVI was computed using reflectance values in the red band (B4) and near-infrared (B8).

Concurrently, shortwave infrared transformed reflectance (STR) was calculated using reflectance values in the SWIR band (B12), following the method outlined by Sadeghi et al. [17] (Table 2).

Table 2
The specification of used satellite images (Sentinel2)

Spectral resolution	**Wavelength (μm) Sentinel2A/B**	**Spatial resolution (m)**
B4 (Red)	0.649 – 0.680 / 0.650 – 0.681	10
B8 (NIR)	0.780 – 0.886 / 0.780 – 0.886	10
B11 (SWIR)	1.568 – 1.659 / 1.563 – 1.657	20
B12 (SWIR)	2.115 – 2.292 / 2.093 – 2.278	20

Results and Conclusions

In the research, we explored the feasibility of a remote sensing-based, soil moisture estimation model, for an area of Hungary, comprised of agricultural fields, with a total expanse of 5500 km^2. The study spans a period characterized by dry and wet conditions. Following the selection of Sentinel2 bands and preprocessing, the OPTRAM model (Equation 4) was parameterized based on the pixel distribution within the STR-NDVI space. During the analysis, dry (i_d and s_d) and wet (i_w and s_w) edges were identified through visual inspection of the STR-NDVI spaces, ensuring that the trapezoids covered the majority of the pixels (Figure 8). It is worth noting that, in all cases, the STR-NDVI space consistently produced trapezoidal shapes, as indicated by the analysis results. The model was executed separately for each selected record, resulting in an estimate of the normalized moisture content (W), as illustrated in Figure 8.

The OPTRAM model proves versatile for calculating the spatial distribution of soil moisture across extensive areas. Furthermore, employing time series analysis enables the mapping of the temporal variation in soil moisture over time.

The study findings illustrate distinct trends in area drying, revealing the rate and progression, from an initial wetter period to a subsequent drier phase. To gain deeper insights, it is recommended to conduct analyses that plot deviations from the mean.

The reliability of the OPTRAM model was evaluated using soil moisture data from 14 drought monitoring stations. The average variance between measured and calculated soil moisture stood at 14%. However, at two stations, the variance was notably high, reaching 33-34%. Upon excluding these outlier stations, the mean difference reduced to 10%.

It is worth noting that the soil at these two outlier stations contains significantly higher levels of CaCO3 compared to other stations: 16-24 m% versus 2-13 m%. Despite this difference, no clear correlation emerged between lime content and calculation accuracy.

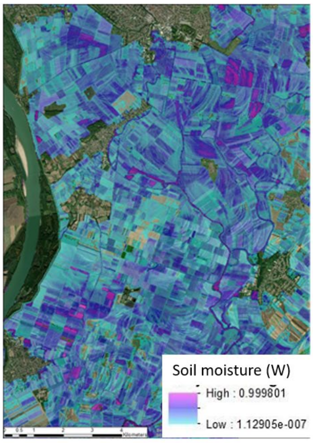

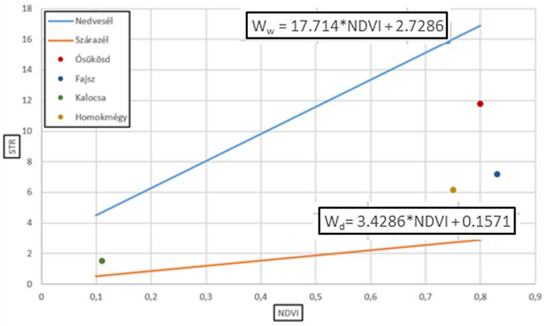

$$W = \frac{0{,}157 + 3{,}429 * NDVI - STR}{0{,}157 - 2{,}729 + (3{,}429 - 17{,}714) * NDVI}$$

Figure 8
Soil moisture variability within study area, determination of the parameters of the OPTRAM procedure for the satellite image of April 2021

In light of the verification results, the OPTRAM model demonstrates efficacy in determining soil moisture. Our analysis achieved a global accuracy of 10% across 14 verification points.

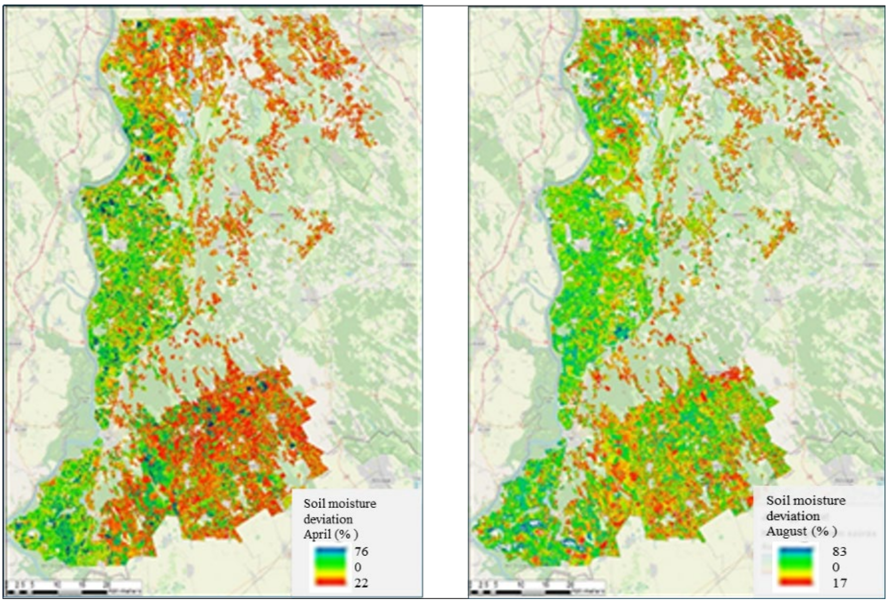

Figure 9
Deviation in soil moisture in 2021 April and (left) and 2021 August (right)

In order to monitor soil dehydration over time, multiple soil moisture deviation maps were generated (refer to Figure 9). Each pixel represented the difference in soil moisture from the average soil moisture. In the figure, soil moisture variance is represented using a color scale: areas with significantly higher-than-average moisture appear in blue, average conditions in yellow, and lower-than-average moisture in red. In April, the Kalocsai-Sárköz and Mohácsi-sziget regions exhibit average to above-average soil moisture levels, while the Solti Plain and the surrounding areas - including the Kiskunság Sand Ridge, the Bácska Loess Plain, and Illancs - show below-average moisture. By August, soil moisture had increased substantially in the eastern part of the Bácska Loess Plain, as well as in the Illancs region and across the entire Solti Plain. The dehydration process in the northern and south-eastern parts was observed over the course of a month.

References

[1] M. Wojtaszek Verőné, V. Szabó, J. Kauser, A. Kocsis and L. Lippmann, Mapping of soil moisture variability within a field by the OPTRAM model. Precision Agriculture’2, Editid by John V. Stafford, Wageningen Academic Publishers, 2021, pp. 459-466

[2] O. S. Ihuoma and Ch. A. Madramootoo, Recent advances in crop water stress detection. Computers and Electronics in Agriculture, 2017, 141 pp. 267-275

[3] H. Jones, Remote sensing of plant stresses and its use in irrigation management, Acta Horticulturae 2012, 1038, pp. 239-247, https://doi.org/10.17660/ActaHortic.2014.1038.28

[4] M. L. Whiting, L. Li, S. L. Ustin, Predicting water content using Gaussian model on soil spectra. Remote Sens. Environ. 89 (4), 535-552 (2004)

[5] H. Zhang, M. Han, J. L. Chavez and Y., Lan Improvement in estimation of soil water deficit by integrating airborne imagery data into a soil water balance model Int. J. Agric. Biol. Eng., 10 (3) pp. 37-46 (2017)

[6] W. W. Verstraeten, F. Veroustraete, C. J. van der Sande, I. Grootaers and J. Feyen, Soil moisture retrieval using thermal inertia, determined with visible and thermal spaceborne data, validated for European forests. Remote Sens. Environ. 101 (3), 299-314 (2006)

[7] L. Hassan-Esfahani, A. Torres-Rua, A. Jensen and M. McKee, Assessment of surface soil moisture using high-resolution multi-spectral imagery and artificial neural networks. Remote Sens. 7 (3), 2627-2646 (2015)

[8] N. N. Das, B. P. Mohanty and E. G. Njoku, Characterization of backscatter by surface features in L-band active microwave remote sensing of soil moisture. IGARSS 2008IEEE International Geoscience and Remote Sensing Symposium. 2 IEE E, pp. II-817 (2008)

[9] I. E. Mladenova, T. J. Jackson, E. Njoku, R. Bindlish, S. Chan, M. H. Cosh, T. R. H. Holmes, R. A. M. De Jeu, L. Jones, J. Kimball and S. Paloscia,

Remote monitoring of soil moisture using passive microwave-based techniques—theoretical basis and overview of selected algorithms for AMSR-E. Remote Sens. Environ. 144, 197-213 (2014)

[10] Z. Dövényi (szerk) K. Rajnai, G. Tóth, T. Tiner, Z. Dövényi, G. Michalkó, Z. Keresztesi, Cadastre of Hungary's Microregions, Geographical Research Institute, Hungarian Academy of Sciences (Magyarország kistájainak katasztere, MTA Földrajztudományi Kutatóintézet), Budapest (2010) ISBN 978-963-9545-29-8

[11] https://atk.hun-ren.hu/en/taki_angol/services/ (http://mta-taki.hu/hu/osztalyok/gis-labor/agrotopo)

[12] R. Nemani, L. Pierce, S. Running and S. Goward, Developing satellite-derived estimates of surface moisture status. J. Appl. Meteorol. 32 (3), 548-557 (1993)

[13] T. N. Carlson, R. R. Gillies and E. M. Perry, A method to make use of thermal infrared temperature and NDVI measurements to infer surface soil water content and fractional vegetation cover. Remote Sens. Rev. 9 (1-2), 161-173 (1994)

[14] A. Ghulam, Q. Qin and Z. Zhan, Designing of the perpendicular drought index. Environ. Geol. 52 (6), 1045-1052 (2007)

[15] Q. Qin, C. Jin, N. Zhang and X. Yang, An two-dimensional spectral space based model for drought monitoring and its re-examination. Geoscience and Remote Sensing Symposium (IGARSS), 2010 IEEE International. IEEE, pp. 3869-3872 (2010)

[16] A. Ghulam, Z. L Li, Q. Qin, Q. Tong, J. Wang, A. Kasimu and L. Zhu, A method for canopy water content estimation for highly vegetated surfaces-shortwave infrared perpendicular water stress index. Sci. China Ser. D Earth Sci. 50 (9) pp. 1359-1368 (2007)

[17] H. Feng, C. Chen, H. Dong, J. Wang and Q. Meng, Modified shortwave infrared perpendicular water stress index: a farmland water stress monitoring method. J. Appl. Meteorol. Climatol. 52 (9), 2024-2032 (2013)

[18] M. Sadeghi, S. B. Jones and W. D. Philpot, A linear physically-based model for remote sensing of soil moisture using short wave infrared bands. Remote Sens. Environ. 164, pp. 66-76 (2015)

[19] L. Aaronm, M. Daigh and G. Peter Oduor, Soil Moisture Mapping with Moisture-Related Indices, OPTRAM, and an Integrated Random Forest-OPTRAM Algorithm from Landsat 8 Images. Remote Sens. 2022, 14(15), 3801; https://doi.org/10.3390/rs14153801

[20] M. Verőné Wojtaszek, I. Abdurahmanov, Crop water condition mapping by optical remote sensing. International Journal of Geoinformatics 17: 1 pp. 11-17 (2021)